MOLECULAR AND CELLULAR BIOLOGY, June 2006, p. 4499–4510 Vol. 26, No. 12
0270-7306/06/$08.00+0 doi:10.1128/MCB.00079-06

Centromeric Histone H3 Is Essential for Vegetative Cell Division and for DNA Elimination during Conjugation in *Tetrahymena thermophila*†

Bowen Cui and Martin A. Gorovsky*

Department of Biology, University of Rochester, Rochester, New York 14627

Received 12 January 2006/Returned for modification 16 March 2006/Accepted 3 April 2006

The *Tetrahymena thermophila CNA1* gene encodes the centromeric H3, Cna1p. Green fluorescent protein (GFP)-tagged Cna1p localizes in micronuclei in dots whose number and behavior during mitosis and conjugation are consistent with centromeres. During interphase, Cna1p-GFP localizes in peripheral dots, suggesting centromeres are associated with the nuclear envelope. Newly synthesized Cna1p-GFP enters micronuclei in mitosis and accumulates in the nucleoplasm. Its deposition at centromeres starts at early S phase and continues through most of S phase. *CNA1* is required for vegetative cell growth. Knockdown of *CNA1* genes in the somatic macronucleus results in micronuclear DNA loss and delayed chromosome segregation during mitosis. During conjugation, Cna1p-GFP disappears from the centromeres in the developing macronucleus, consistent with centromeric sequences being internal eliminated sequences. Surprisingly, zygotic *CNA1* is required for efficient elimination of germ line-specific sequences during development of the new macronuclei but not for the RNA interference pathway, through which sequences are targeted for elimination. Zygotically expressed Cna1p localizes in the spherical structures in which the later stages of DNA elimination occur, and these structures cannot be formed in the absence of zygotic *CNA1*, suggesting that, in addition to functioning in centromeres, Cna1p may also play a role in organizing the formation of the DNA elimination structures.

Histones are the architectural proteins that compact DNA into chromatin, and considerable evidence supports the view that covalent modifications of histones and histone variants contribute to nucleosome functional heterogeneity and play important roles in chromatin regulation (for a review, see reference 28). All eukaryotes analyzed to date contain centromere-specific histone H3 variants, termed CenH3s (15, 21, 30, 32, 35, 36). CenH3s are chimeric proteins, consisting of a C-terminal domain that is homologous to the conserved histone fold domain (HFD) of noncentromeric H3s and a nonhistone N-terminal region that differs in length and sequence in different eukaryotes (Fig. 1A and B). In vivo, CenH3 homotypic nucleosomes associate with centromeric DNA in place of the typical H3s associated with the rest of the genome. The conserved HFD of CenH3 likely performs structural functions similar to the HFDs of other H3s (4) and also is required for targeting CENP-A to the centromere in mammalian cells (37). The precise functions of the divergent N termini are unknown, although it has been suggested that they interact with other centromeric proteins and may play a role in evolutionary suppression of meiotic drive (38). Despite their divergent N termini, CenH3s are functionally conserved (41). They are required for functional centromeres and for recruitment of other centromeric and spindle checkpoint proteins. Mutations in CenH3s result in mitotic arrest and/or extensive chromosome mis-segregation.

The timing of centromere DNA replication and of CenH3 deposition into centromeres varies in different organisms. In human cells, centromere DNA replicates in late S phase, and CENP-A is synthesized in G_2 (31). In *Drosophila melanogaster*, different procedures used to study centromere replication indicated that it occurs either at early or late S phase (1, 34). Cid, the *Drosophila* CenH3, can be deposited in centromeres independent of DNA replication throughout the cell cycle (1, 2).

We and others (6) identified a putative centromere H3 gene in the recently completed sequence of the *Tetrahymena thermophila* macronuclear genome (http://www.tigr.org/tdb/e2k1/ttg/). As is characteristic of ciliated protozoans, each *Tetrahymena* cell has two nuclei (16), a diploid germ line micronucleus (MIC) and a polyploid (~45C) somatic macronucleus (MAC). During asexual reproduction (vegetative growth), the MIC divides mitotically without nuclear membrane breakdown (closed mitosis), and it is transcriptionally inert. The MAC divides amitotically, a process in which chromosomes behave as if they are acentric and are distributed randomly to daughter cells. The transcriptionally active MAC is responsible for all of the gene expression in the vegetative cell. Sexual reproduction (conjugation) of *Tetrahymena* can be initiated by mixing starved cells of different mating types. During conjugation, the MICs undergo meiosis, prezygotic mitosis, fertilization, and two postzygotic mitoses to produce four identical nuclei, two of which develop into the new MICs of the progeny cells; the other two enlarge and develop into the new MACs (NMs). As the NMs develop, transcription is initiated from the zygotic genome, and the old parental MACs (OMs) stop transcribing and undergo an apoptosis-like degradation. If refed, cells that finish conjugation (exconjugants) resume vegetative growth.

During NM development, the genome undergoes breakage accompanied by small amounts of DNA elimination and telomere addition at ~250 breakage elimination sites (BESs) and ~6,000 interstitial deletions of internal eliminated sequences (IESs), resulting in elimination of about 15% of the MIC genome. Recent studies have shown that IESs are targeted for

* Corresponding author. Mailing address: Department of Biology, University of Rochester, Rochester, NY 14627. Phone: (585) 275-6988. Fax: (585) 275-2070. E-mail: goro@mail.rochester.edu.

† Supplemental material for this article may be found at http://mcb.asm.org.

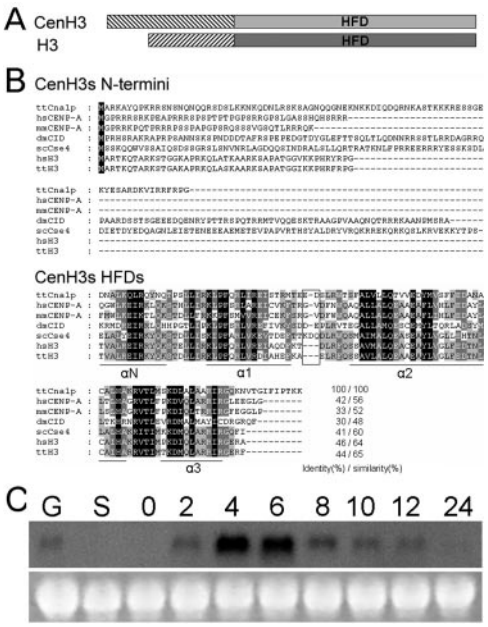

FIG. 1. Characterization of *CNA1*. (A) The schematic drawing shows that CenH3 has a histone fold domain (HFD) that shares high homology with H3 and an N-terminal region that is very diversified. (B) Centromere H3 proteins. tt, *Tetrahymena thermophila*; hs, *Homo sapiens*; mm, *Mus musculus*; dm, *Drosophila melanogaster*; sc, *Saccharomyces cerevisiae*. The sequences of *Tetrahymena* H3 (ttH3) and human H3 (hsH3) are included for comparison. The top panel shows the N-terminal regions of the proteins which have almost no homology. The bottom panel is the alignment of the HFDs of the proteins; the identity and similarity of a protein compared to ttCna1p are indicated. αN, α1, α2, and α3 indicate the α-helixes in the histone fold domains. The boxed area indicates the longer L1 loop in the CenH3s compared to those of H3s. (C) Expression pattern of the *CNA1* gene. Total RNA from wild-type log-phase growing (G), starved (S), and conjugating cells (0, 2, 4, 6, 8, 10, 12, and 24 h postmixing) were used. The upper panel is the Northern blot probed with *CNA1* coding sequence. The lower panel is the loading control of rRNA stained with ethidium bromide before blotting.

DNA elimination by a process that is similar to heterochromatin silencing in other organisms (22, 39), which involves an RNA interference (RNAi) machinery that targets the histones associated with specific sequences to become methylated at histone H3 K9 and associated with chromodomain proteins (for a review, see reference 24).

Here we describe the properties of *Tetrahymena* centromeric H3, Cna1p. Green fluorescent protein (GFP)-tagged Cna1p localizes as peripheral dots in interphase MICs, and the behavior of these dots during mitosis and meiosis argues strongly that Cna1p is a centromere protein. Accumulation of induced Cna1p-GFP in micronuclei starts in M phase, but its localization to centromeres is S phase specific. The disappearance of centromeric Cna1p-GFP from developing MACs during conjugation is consistent with centromeric sequences being IESs. *CNA1* is shown to be essential for both vegetative growth and conjugation. Incomplete somatic knockout of *CNA1* results in delay of chromosome segregation and a small MIC phenotype, indicative of DNA loss. Surprisingly, during conjugation, zygotic expression of Cna1p is required for DNA elimination. In conjugating cells in which the *CNA1* gene has been knocked out in micronuclei but not in the parental macronuclei, scan RNAs (scnRNAs) accumulate, histone H3 K9 methylation occurs, and the chromodomain protein Pdd1p appears in developing MACs, but the DNA elimination structures are not formed. In wild-type cells, Cna1p is detected in the DNA elimination structures using a specific antibody against Cna1p (α-Cna1p [6]). These results indicate that Cna1p plays a critical role in later stages of DNA elimination, and centromere regions may function as the initiation sites for the formation of DNA elimination structures.

MATERIALS AND METHODS

***Tetrahymena* strains and culture conditions.** Wild-type CU428 and B2086 strains of *Tetrahymena thermophila* were provided by Peter J. Bruns (Cornell University). Cells were grown in 1× super protease peptone (SPP) medium at 1% proteose peptone (13) at 30°C. To induce conjugation, mid-log-phase growing cells of different mating types were starved for 22 to 24 h at 30°C in 10 mM Tris (pH 7.5) and mixed together.

Cloning the *CNA1* gene. A gene encoding a putative CenH3 was identified in the *Tetrahymena thermophila* database (http://www.tigr.org/tdb/e2k1/ttg), and a PCR product containing a 0.9-kb 5′ flanking region, a 564-bp *CNA1* coding region, and a 1.9-kb 3′ flanking region was amplified from genomic DNA. The product was digested by AccI and PstI and cloned into Bluescript KS$^+$ vector (Stratagene). The construct was named pCNA1 and verified by sequencing. The accession number of *CNA1* in GenBank is DQ126145.

Construction of the *MTT1-CNA1-GFP* strain. A pTTMet construct (29) containing 489 bp *MTT1* coding sequence, ~2 kb 5′ flanking sequence, and ~400 bp 3′ flanking sequence was used to create the *MTT1-CNA1-GFP* construct. A *neo2* cassette (12) was inserted into the 5′ flanking sequence of the pTTMet construct ~900 bp upstream of the start codon as a selectable marker. The *MTT1* coding sequence in the resulting construct was then replaced by the *CNA1-GFP* sequence consisting of the *CNA1* coding sequence, a 6-amino-acid linker encoded by TCTAGGCCTGTTGCTACT, and the *GFP* coding sequence. The construct was then transformed into the macronuclear *MTT1* locus of CU428 and B2086 by biolistic transformation (5) to give *MTT1-CNA1-GFP* (MCG) cell strains.

For localization of Cna1p-GFP protein in growing cells, MCG cells in which the *MTT1* gene had been partially replaced were grown in 200 μg/ml paromomycin (pm), 0.5 μg/ml Cd^{2+} SPP medium overnight to mid-log phase, fixed in 0.5% formaldehyde at room temperature for 5 min, and resuspended in phosphate-buffered saline (PBS) with 0.1 μg/ml 4′,6′-diamidino-2-phenylindole (DAPI) (Roche). Eight sections through the nuclei were obtained by confocal microscopy (Leica TCS SP), and the overlaid images are shown in the figures.

For localization of Cna1p-GFP protein in conjugating cells, MCG cells of different mating types were grown in 200 μg/ml pm, 0.5 μg/ml Cd^{2+} SPP overnight to mid-log phase, washed twice with starvation medium (10 mM Tris, pH 7.5), kept starved without addition of Cd^{2+} for 24 h, mixed, fixed, and photographed at different stages. Addition of Cd^{2+} before conjugation gave similar results.

To study the deposition of Cna1p-GFP in growing cells, MCG cells were grown in 200 μg/ml pm without Cd^{2+} to mid-log phase. Cd^{2+} was added to 1 μg/ml, and the deposition of newly synthesized Cna1p-GFP was monitored. For starved cells, MCG cells were grown in 200 μg/ml pm without Cd^{2+} to mid-log phase and starved in 10 mM Tris (pH 7.5) for 24 h. Cd^{2+} was added to 0.06 μg/ml, and the deposition of newly synthesized Cna1p-GFP was analyzed.

For all localization and deposition studies of Cna1p-GFP, living cells were observed, and results obtained were similar to those from the fixed cells.

Construction of somatic *CNA1* knockouts. The *CNA1* knockout construct was created by replacing the 564-bp *CNA1* coding sequence in pCNA1 with the *neo2* cassette. The construct was transformed into the macronuclear *CNA1* locus by biolistic transformation. The transformants were assorted to the highest concentration of pm (1.2 μg/ml) at which cells would grow. Incomplete somatic *CNA1* knockout strains (i-Δs*CNA1*) were then established from single cells.

Construction of germ line *CNA1* knockouts. The same knockout construct described above was transformed into the micronuclear *CNA1* locus of mating B2086 and CU428 cells, and homozygous *CNA1* knockout heterokaryons (Δg*CNA1*) were obtained as described previously (14).

Analysis of small RNA. Total RNA was extracted with TRIzol reagent (Invitrogen), separated on 12% polyacrylamide-urea DNA sequencing gels, and visualized as described previously (22).

Analyses of M element processing. Cells were collected from mass matings of wild-type or Δg*CNA1* cells and lysed as previously described (17). The lysate was used directly for the PCR. The primers used for the PCR analysis were the following (nucleotide position and direction): M5′ (2 to 25, sense) and M3′ (1172 to 1194, antisense). The GenBank accession number of the M element is M21936.

Analyses of BES-Tt819 region processing. Wild-type or Δg*CNA1* cells were mated, and single-cell PCR was performed on single exconjugants as previously described (22). Primers 819-1 (nucleotide positions 481 to 503, antisense), 819-4 (1 to 26, sense), and Tel (CCCCAACCCCAACCCCAA) were used for the first PCR. 819-2 (453 to 476, antisense), 819-3 (52 to 77, sense), and Tel were used for the second PCR. The GenBank accession number of the Tt819 region is V00618.

Indirect immunofluorescence analysis. For Pdd1p staining, cells were fixed in Lavdowsky's fixative (50:10:1:39 ethanol:formaldehyde:acetic acid:water) overnight at 4°C and dried onto poly-L-lysine-coated coverslips. They were then incubated with α-Pdd1p polyclonal antibody (1:200 dilution; provided by C. David Allis, The Rockefeller University, New York, NY) in blocking solution (10% normal goat serum, 3% bovine serum albumin, 0.1% Tween-20 in PBS) overnight at 4°C, followed by incubation with fluorescein isothiocyanate-conjugated goat anti-rabbit secondary antibody (1:200 dilution; Zymed Laboratories). The samples were incubated with 10 ng/ml DAPI (Roche) in PBS, mounted, and imaged by confocal microscopy (Leica TCS SP).

For H3 K9 methylation staining, cells were fixed in Schaudin's fixative (saturated $HgCl_2$ [0.074 g/ml] and 100% ethanol at a 2:1 dilution) at room temperature for 5 min, washed with methanol twice, and dried onto poly-L-lysine-coated coverslips (19). The coverslips were then incubated with α-H3 K9 dimethylation antibody (1:50 dilution; Upstate Biotechnology) in blocking solution (10% normal goat serum in Tris-buffered saline [TBS]) overnight at 4°C, followed by incubation with fluorescein isothiocyanate-conjugated goat anti-rabbit secondary antibody (1:200 dilution; Zymed Laboratories). The samples were incubated with 10 ng/ml DAPI in TBS, mounted, and imaged by confocal microscopy (Leica TCS SP).

RESULTS

Characterization of the *CNA1* gene. A putative *Tetrahymena* CenH3 gene (*CNA1*) was identified by searching the *Tetrahymena* genome database using *Tetrahymena* histone H3 as the query. Alignment of *Tetrahymena* Cna1p, H3, and CenH3 proteins of other organisms (Fig. 1B) demonstrates that Cna1p has an HFD with high homology to the H3 HFD and a diverged N-terminal domain. Like CenH3s of other organisms, the HFD of *Tetrahymena* Cna1p contains additional amino acids in the loop (L1) between α-helix I and II compared to histone H3.

CNA1 was expressed (Fig. 1C) at a low level in vegetative growing cells, was not detectable in starved cells, and was expressed in conjugating cells, especially strongly at 4 to 6 h postmixing. This expression pattern is consistent with Cna1p function in centromere formation: Cna1p functions in growing cells when MICs are replicating, does not function in starved cells when MICs are arrested at G_2 phase, and functions during conjugation when MICs undergo three rapid mitoses (one prezygotic and two postzygotic) within ~2 h.

Cna1p-GFP localization in vegetative cells demonstrates it is a centromere protein. To study Cna1p localization and deposition, *CNA1-GFP*, with a GFP coding sequence inserted at the C terminus of the *CNA1* open reading frame, was used to replace the MAC Cd^{2+}-inducible metallothionein gene (*MTT1* [29]) coding sequence, creating somatic MCG (*MTT1-CNA1-GFP*) strains (Fig. 2A).

In MCG cells grown with Cd^{2+} overnight, Cna1p-GFP localized mainly in small green dots at the periphery of MICs (Fig. 2B), suggesting that centromeres are associated with the MIC nuclear envelope. There are 10 chromosomes in a diploid *Tetrahymena* MIC. The number of dots that could be counted in nondividing MICs was mostly fewer than, but close to, 10 (Fig. 2B and C, a). Occasionally 10 were resolvable (see Fig. 4A, a), but never more than 10. These observations indicate some centromeres may cluster. The absence of GFP signals in MACs is consistent with the view that *Tetrahymena* MAC chromosomes are acentric.

Figure 2C shows the behavior of Cna1p-GFP-labeled dots in MICs during the closed MIC mitosis. At prophase, the MIC elongated and the Cna1p-GFP-labeled dots were relocalized toward the center of the nucleus (Fig. 2C, b). In some dividing MICs, the dots were lined up in the middle of the nucleus as if in a metaphase plate (Fig. 2C, c). This result is consistent with the observation that what appear to be kinetochore microtubule bundles are arranged peripherally around the chromatin mass at early metaphase and are localized in the center of the nucleus at later metaphase (10). At anaphase, the dots localized to the pole-proximal edge of the dividing MICs (Fig. 2C, d). In many anaphase MICs, the dots appeared smaller and the total number in each separated set was close to 10, consistent with separation of sister centromeres. At telophase, the dots partially coalesced at the pole-proximal region of the divided MICs (Fig. 2C, e). As MICs completed mitosis, they immediately entered S phase (44). At the same time, the MAC elongated and started dividing (Fig. 2C, f and g). Immediately before and after MICs complete mitosis, it was often possible to count 5 distinct dots, indicating that somatic pairing of homologous centromeres had occurred. While the MAC was dividing, the Cna1p-GFP-labeled dots stayed at one side of the MIC (Fig. 2C, f to h), and this configuration was observed in most nondividing interphase cells as well (Fig. 2B and C, i), indicating that centromeres remain associated, as in the Rabl orientation found in other cell types (see Fig. 390 of reference 42).

The number and behavior of Cna1p-GFP-labeled dots in interphase and during mitosis is consistent with the expected properties of centromeres, strongly arguing that Cna1p is the centromeric H3 in *Tetrahymena*. We also noted that MCG cells have a weak Cna1p-GFP signal throughout the micronucleus during M and S phases that was higher than the "background" signal in interphase MICs. While we cannot rule out the possibility that this signal is also chromosomal, it appears to be mainly nucleoplasmic, as indicated by the fact that it can be observed in the thin "central spindle"-like region that connects daughter micronuclei before they separate completely and lacks detectable DNA staining (Fig. 2C, e). This nucleoplasmic signal likely represents the early accumulation of newly synthesized Cna1p that is needed for centromere replication during S phase (see below).

Accumulation of newly synthesized Cna1p-GFP in MICs starts before S phase, while deposition of Cna1p-GFP into centromeres occurs during S phase. Micronuclei and macronuclei have nonoverlapping S phases and divide at slightly different times in the cell cycle. MICs divide before MACs, which divide during cytokinesis. MICs initiate replication immediately after they divide (there is no detectable MIC G_1 phase), continue replicating during MAC division/cytokinesis, and finish shortly after the cell divides (43, 44). Nondividing, G_2 MICs are round and are positioned near MACs. Dividing M-phase MICs can be identified by their elongated shape and their positions away from MACs. To analyze when Cna1p is

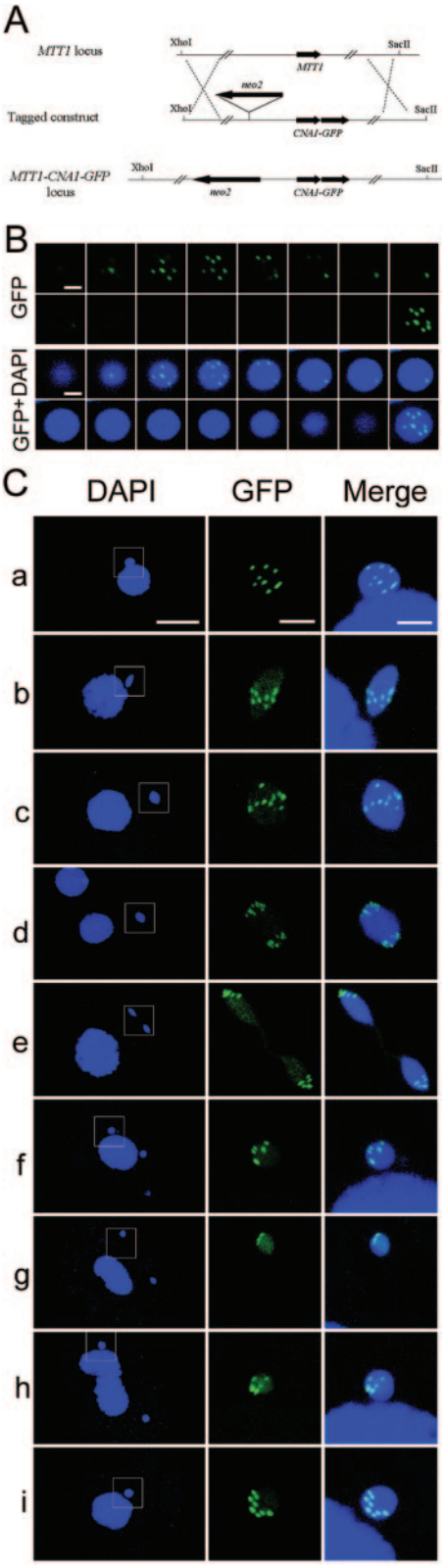

FIG. 2. Localization of Cna1p-GFP protein in vegetative growing cells. (A) Diagram of the *CNA1* GFP-tagged construct at the *MTT1* locus. *MTT1* coding sequence was replaced by *CNA1-GFP* coding sequence. The *neo2* selectable marker was inserted into the 5′ flanking region of the *MTT1* locus ~900 bp upstream of the start codon. (B) Cna1p-GFP is localized as peripheral dots in MIC. Fifteen sequential cofocal images through a MIC with intervals of 0.28 μm, as well as the overlaid image (the last image in each panel), are shown. Scale bar, 2 μm. (C) Localization of Cna1p-GFP in log-phase cells. The first column is DAPI staining of the cells at lower magnification. Scale bar, 20 μm. The second (GFP) and third columns (merge of GFP and DAPI) are 4× magnifications of the boxed area indicated in the first column. Scale bars, 4 μm. Each picture shown is an overlaid image of eight sections through the nuclei obtained by confocal microscopy. a, interphase cell; b, MIC prometaphase; c, MIC metaphase; d, MIC anaphase; e, MIC telophase/start of S phase; f, MIC S phase, early MAC elongation; g and h, MIC S phase and MAC division; and i, interphase cell.

deposited in the centromere region during the cell cycle, Cna1p-GFP expression was induced by adding Cd^{2+} to either growing or starved MCG cells. In growing cells, 2 h after induction most interphase cells (mostly in MIC G_2) were unlabeled (Fig. 3A, b). M-phase MICs exhibited a strong nucleoplasmic signal, but no GFP-labeled dots were observed (Fig. 3A, c and d), indicating that Cna1p-GFP could enter M but not G_2 MICs, and it was not deposited into centromeres. In contrast, strongly labeled Cna1p-GFP dots were observed in all MICs that are in S phase (Fig. 3A, e to g). In starved cells (Fig. 3B) in which MICs are arrested at G_2, the MIC nucleoplasm labeled strongly 10 h after induction, but no Cna1p-GFP-labeled centromere dots were observed (Fig. 3B, b). These studies argue that Cna1p-GFP deposition into centromeres is S phase specific, but its synthesis and import into MIC starts in M phase, before its deposition.

Cna1p localization during conjugation. During early conjugation, the MIC undergoes meiosis. The first detectable stages of meiosis occur when the MIC starts to elongate into a teardrop-shaped structure in which telomeres have been localized to the relatively DNA-rich end (18); Cna1p-GFP-labeled dots were all localized at the DNA-poor end (Fig. 4A, b). As the MIC continues to elongate into a torch-shaped structure, where telomeres have been localized to the tip of the narrow elongated end (18), Cna1p-GFP-labeled dots were localized at the tip of the other, wide end (Fig. 4A, c). When the MIC is fully elongated into the "crescent" stage, the Cna1p-GFP-labeled dots were all localized at one tip of the crescent (Fig. 4A, d). Thus, the organization of the crescent-stage nucleus in *Tetrahymena* is similar to the horsetail stage of meiotic chromosome pairing in *Schizosaccharomyces pombe* (8) and the bouquet stage of meiosis observed in many organisms (see Fig. 48-3 in reference 27). This combination of telomeres clustered at one end and centromeres clustered at the other, coupled with extreme extension of the crescent micronucleus, likely enables efficient pairing of meiotic homologues in the absence of a synaptonemal complex (18).

As conjugation proceeds through the two meiotic divisions, the haploid prezygotic mitosis and the two postzygotic mitotic divisions, centromeric dots were detected in the nuclei, but the nucleoplasm also acquired a strong GFP signal (Fig. 4A, e to m). The likely explanation for this nuleoplasmic signal is that MICs may be accumulating Cna1p in preparation for the rapid mitotic divisions that occur within the following 2 h, just as MICs in growing cells accumulate Cna1p in M phase prior to deposition in S phase.

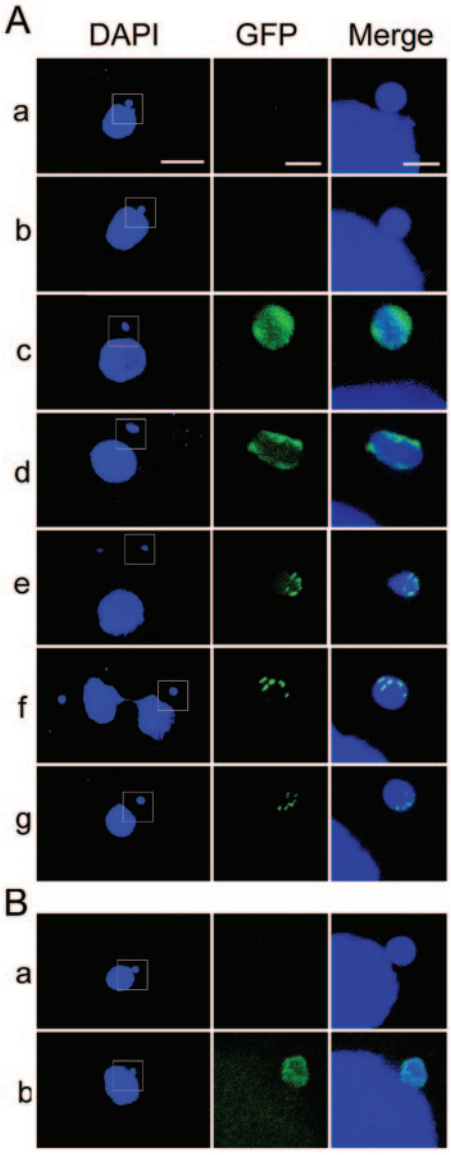

FIG. 3. Cna1p-GFP deposition. The arrangement and magnifications are the same as those described in the legend to Fig. 2C. (A) Cna1p-GFP is deposited into centromeres during S phase. a, a growing MCG cell before induction of Cna1p-GFP expression; b to g, 2 h after induction; b, an unlabeled interphase cell; c and d, MIC M phase; e to g, MIC S phase. (B) Cna1p-GFP cannot be deposited into centromeres in starved cells in which the MICs are arrested at G_2 phase. a, starved MCG cell before induction; b, 10 h after induction.

After the second postzygotic division, the two micronuclei in the anterior of the cell begin to enlarge and differentiate into NMs. When differentiation of the NM begins, its zygotic genome starts to express and the OMs cease transcription, become pycnotic, and eventually disappear. As the NMs started to enlarge, the Cna1p-GFP-labeled centromeres were often paired (Fig. 4A, n), indicating homologous chromosomes were paired. As the NMs developed, the centromeric fluorescence in NMs diminished and eventually disappeared, indicating the centromere structures were disrupted. (Fig. 4A, o and p). In contrast, centromeres in the adjacent new MICs continued to fluoresce intensely. The diffuse GFP signal in the nucleoplasm of the developing MACs also decreased and disappeared but was retained longer than the nucleoplasmic signal in the new MICs, likely due to the breakdown of the MAC centromeres. Developing MACs completely lost all detectable GFP signal before pair separation, while the new MICs retained strong centromeric fluorescence (Fig. 4A, q to t), indicating that Cna1p deposited into the MIC centromeres is stable and turns over slowly, if at all. The above observations argue that centromere loss in the developing MAC is an active process. Along with the fact that there are no centromeres in vegetative MACs, it is very likely that centromere DNA sequences are eliminated as IESs in the developing NM after the centromere structures are disrupted.

Because the GFP-tagged *CNA1* gene was inserted into the OM, which becomes transcriptionally silent and is then destroyed during late conjugation, all Cna1p-GFP was expressed parentally from the OM. Thus, it was not possible to study the zygotic synthesis of Cna1p by the methods described above. When wild-type conjugating cells were stained with α-Cna1p antibody (for properties of the antibody, see reference 6), similar Cna1p localization was observed until the 2MAC-2MIC exconjugant stage (see Fig. S1h in the supplemental material). However, in exconjugants, the spherical DNA elimination structures in some cells (~5% of exconjugants) were stained by α-Cna1p antibody (Fig. 4B). Importantly, such localization was never observed with parentally expressed Cna1p-GFP. These observations indicate that zygotically expressed Cna1p can enter the DNA elimination structures in the developing MAC and suggest it could have a role in the DNA elimination process.

***CNA1* is essential for vegetative growth and for maintenance of micronuclear chromosomes.** In vegetatively growing cells, the MIC is transcriptionally inert, and all proteins, including those localized specifically in the MIC, are derived from expression of the somatic MAC genome. To study the function of Cna1p during vegetative growth, the MAC *CNA1* gene coding sequence was replaced by the *neo2* cassette (Fig. 5A) to create somatic *CNA1* knockout cells. Because the MAC is polyploid and divides amitotically, after prolonged selection it is possible to obtain cells in which MAC genes have been completely replaced (if the gene is not essential) or partially replaced (if the gene is essential). Cells in which all of the *CNA1* genes in the MAC were replaced by *neo2* could not be obtained (Fig. 5B), indicating that the *CNA1* gene is required for vegetative growth. In partial *CNA1* "knockdown" cells (i-Δs*CNA1*, incomplete deletion of the somatic *CNA1* genes), MICs were smaller than in wild-type cells (Fig. 5C, a). In these cells, the dividing MIC often was spindle shaped while still closely associated with the MAC, instead of after moving away from the MAC as in wild-type cells (Fig. 5C, b). In wild-type cells with highly elongated, dividing MICs, sister chromosomes were completely separated, while in i-Δs*CNA1* cells with similarly or even more elongated MICs, DAPI staining was often found in the region connecting the daughter nuclei, indicating that separation of sister chromatids was delayed or prevented (Fig. 5C, c). Eventually MICs appeared to be able to complete division but often with unequal partition of DNA to daughter nuclei (Fig. 5C, d and e). These observations are consistent with an

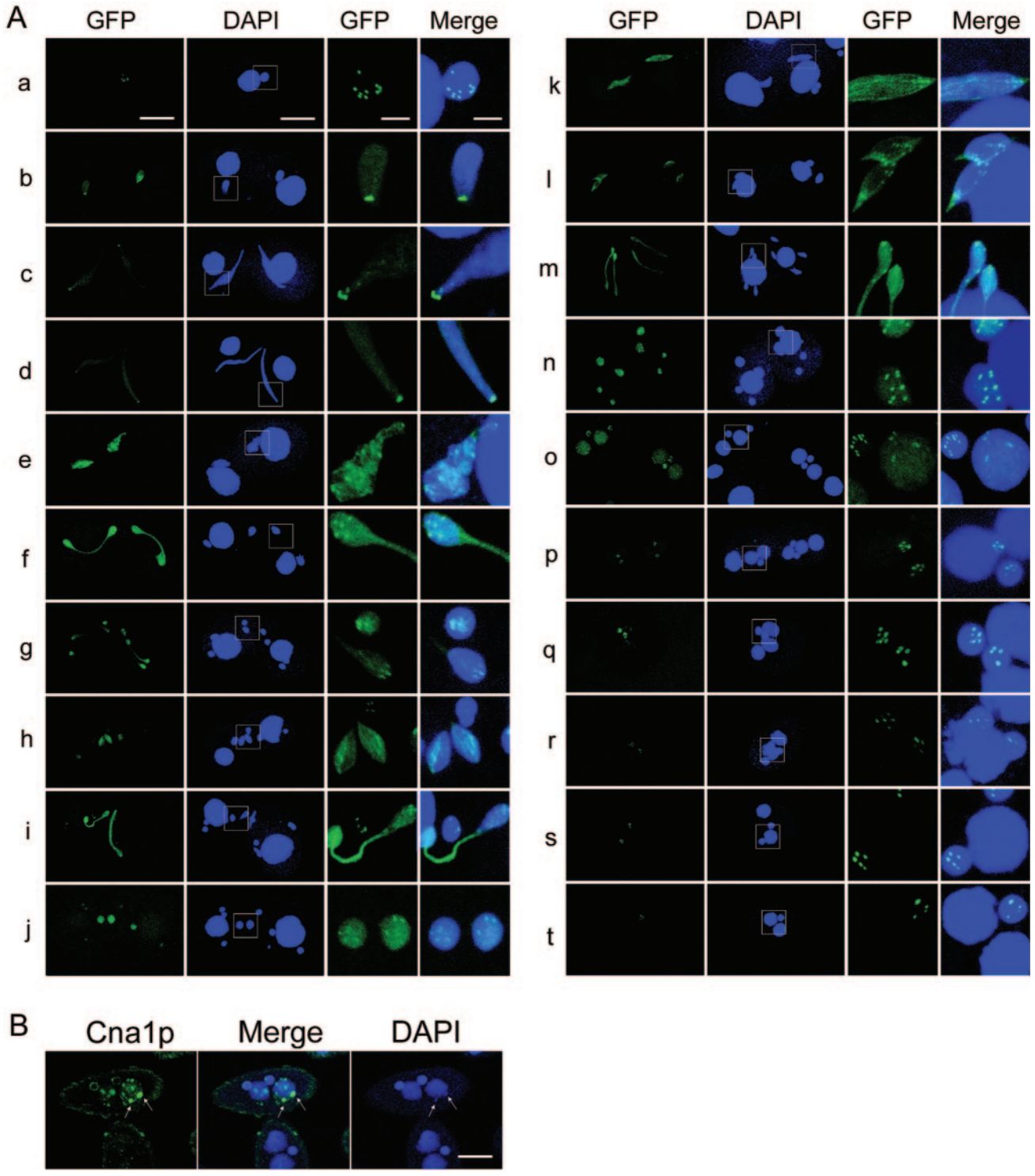

FIG. 4. Localization of Cna1p in conjugating cells. (A) Localization of Cna1p-GFP. The first and second columns are GFP fluorescence and DAPI staining of the cells at lower magnification. Scale bars, 20 μm. The third (GFP) and fourth (merge of GFP and DAPI) columns are 4× magnifications of the boxed areas indicated in the second column. Scale bars, 4 μm. a, starved cell; b, early conjugation; c and d, crescent; e, early first meiotic division; f, first meiotic division; g, second meiotic division; h and i, prezygotic division; j, pronuclear exchange; k, nuclear fusion and first postzygotic division; l, anaphase of second postzygotic division; m, end of second postzygotic division; n, early MAC development; and o to t, late stages in MAC development. (B) Cna1p is localized in the DNA elimination structures. Wild-type cells were fixed at 13.5 h postmixing and were stained using anti-Cna1p antibody as described previously (6). Arrows indicate two DNA elimination structures in NM. Note that the Cna1p colocalizes with the DAPI-stained DNA elimination structures. Scale bar, 12 μm.

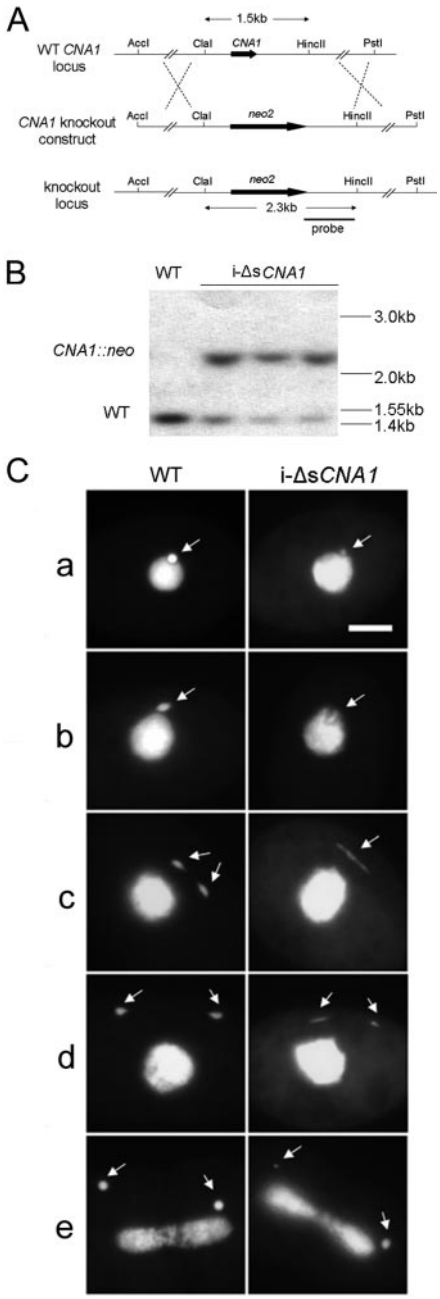

FIG. 5. Macronuclear *CNA1* gene is essential for vegetative growth and is required for proper chromosome segregation and MIC maintenance. (A) Diagram of the *CNA1* knockout construct and the wild-type *CNA1* locus. The *CNA1* coding sequence is replaced by the *neo2* cassette. The probe used for panel B is indicated. (B) Southern hybridization of the incomplete somatic *CNA1* knockout strains (i-Δs*CNA1*). Genomic DNA isolated from wild-type cells (WT) and i-Δs*CNA1* cells (assorted to the highest nonkilling concentration of paromomycin) was digested with ClaI and HincII and hybridized with the probe indicated in panel A. (C) Delayed chromosome segregation and small-MIC phenotype of i-Δs*CNA1* cells. Growing wild-type (WT) or i-Δs*CNA1* cells were fixed and stained with DAPI. Scale bar, 10 μm. Arrows indicate MICs.

essential role of Cna1p, the *Tetrahymena* centromeric H3, in centromere biogenesis and/or function.

Zygotic expression of *CNA1* is required to produce viable conjugation progeny. Germ line *CNA1* knockout homozygous heterokaryon strains (Δg*CNA1*, deletion of germ line *CNA1* gene) were created in which both copies of the *CNA1* gene were disrupted in the MIC, while the MAC *CNA1* genes were wild type (Fig. 6A). When Δg*CNA1* cells were mated, the increased *CNA1* expression observed in late wild-type conjugating cells (Fig. 6B, WT 12 to 16 h) was not observed, demonstrating that this up-regulation of *CNA1* expression is from the zygotic genome in wild-type cells. The earlier stages of conjugation of Δg*CNA1* cells proceeded slightly more slowly than that of wild-type cells (see Fig. S2 in the supplemental material, 3 and 6 h). At later stages, when wild-type cells underwent pair separation, OM degeneration, and destruction of one MIC, the Δg*CNA1* cells remained pairs even after their OMs degenerated (see Fig. S2 in the supplemental material, 9 to 24 h). Δg*CNA1* progeny cells were arrested as exconjugants with two developing MACs and two MICs in either growth medium or in 10 mM Tris, and no viable progeny was obtained. These observations suggest that zygotic expression of *CNA1* is essential for late stages of conjugation and/or the development of exconjugants.

Zygotic *CNA1* is required for efficient DNA elimination. To characterize the nature of the requirement for zygotic expression of *CNA1* to complete conjugation, we examined the progeny of mated Δg*CNA1* cells. When maintained under starvation conditions, developing MACs in wild-type *Tetrahymena* progeny undergo two DNA endoreplications from 2C to 8C (11). The first endoreplication occurs after the second postzygotic mitosis as the new MACs swell. The second occurs in exconjugants when the DNA elimination structures are formed (3). Because the size of the NMs changes little after the initial swelling, the second endoreplication was visually detectable when wild-type cells were stained with DAPI (Fig. 6C, compare 14- and 18-h WT NMs). In Δg*CNA1* exconjugants, this increase of DNA content was not observed. In addition, small aggregates of DAPI staining were observed in the developing MACs of Δg*CNA1* cells (Fig. 6C, Δg*CNA1*) that were never seen in wild-type cells. Some mutations that prevent *Tetrahymena* DNA elimination also arrest cells at the 2MAC-2MIC stage and block endoreplication (24). Coupled with the localization of Cna1p in the DNA elimination structures, these observations suggested that the exconjugants of the mated Δg*CNA1* cells might have a DNA elimination defect and that the heterochromatin-like DAPI-stained aggregates might reflect IESs that failed to be eliminated.

To test this hypothesis, we determined whether the DNA elimination process was affected when zygotic *CNA1* was knocked out. Two well-studied DNA elimination elements, one IES and one BES, were analyzed. Elimination of M element IESs can occur at two alternative breakage-rejoining sites to produce a long or a short form at about equal frequencies (3). Wild-type and Δg*CNA1* cells that were assorted to homozygous short forms in their MACs were mated and analyzed for the appearance of the long form in the exconjugants by PCR, using primers flanking the M element (9) (Fig. 6D, upper panel). If the M element is processed normally, the long form should be detected in addition to the short form, which is much more prevalent, because it preexisted in the OMs of all conjugating cells and in non-maters. If IES elimination does not occur, the M element should not be processed and the long form should not be detected. In a mass mating of wild-type

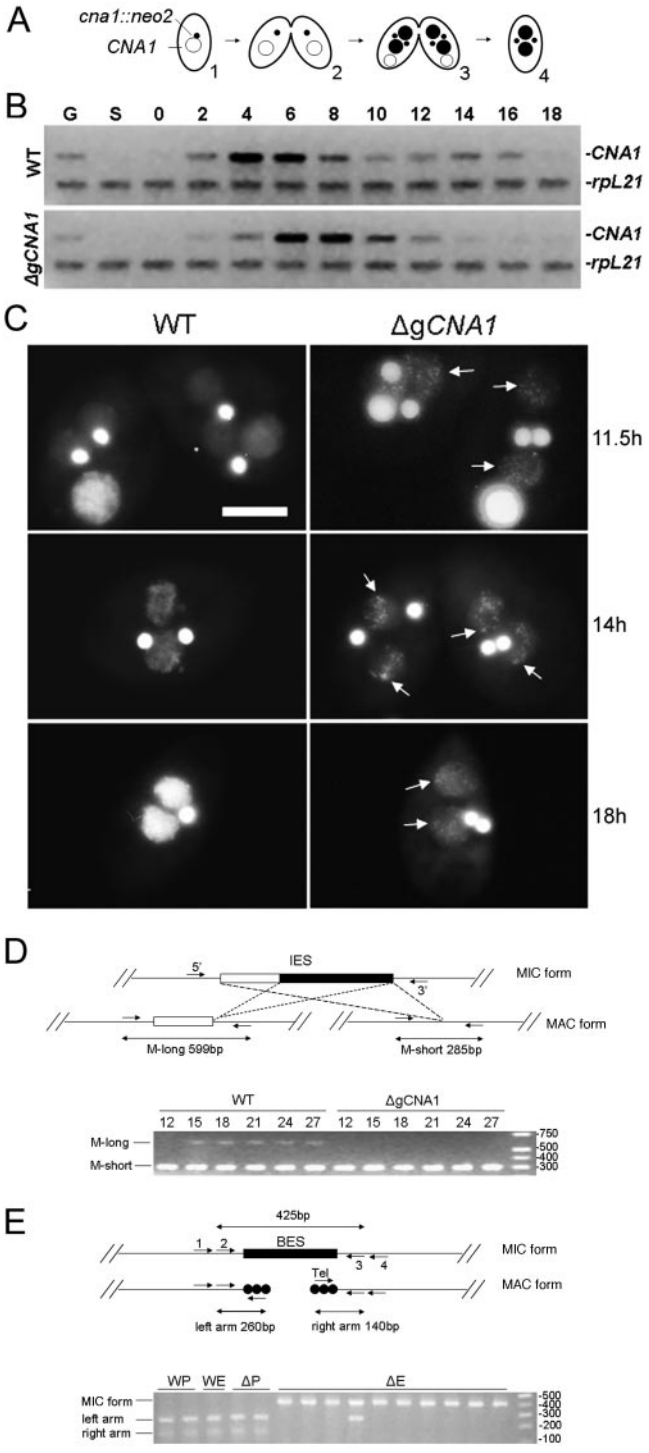

FIG. 6. DNA elimination is defective in conjugated germ line *CNA1* knockout (Δg*CNA1*) cells. (A) Schematic drawing of the mating process of Δg*CNA1* cells. In Δg*CNA1* heterokaryon cells, *CNA1* genes are disrupted by the *neo2* cassette in MIC but are wild type (WT) in MAC (1). When two such cells mate, they form a conjugating pair (2). The conjugating pair then develops to NM stage (3), when the old parental MAC stops transcription and starts degrading, and the new MACs, containing the same zygotic genome as the new MICs, start transcription. The conjugating pair then separates and gives rise to two exconjugants (4). (B) The zygotic *CNA1* expression is up-regulated during late conjugation. The expression of the *CNA1* gene was analyzed by reverse transcription-PCR, amplifying *CNA1* and *rpL21* (loading control) cDNAs at indicated time points. The up-regulation of *CNA1* expression at 12 to 16 h in WT cells is not observed in Δg*CNA1* cells. (C) Endoreplication failure and aggregated chromatin in Δg*CNA1* cells. WT or Δg*CNA1* mating cells were fixed and stained with DAPI at the indicated time postmixing. Scale bar, 10 μm. Arrows indicate the aggregated chromatin in Δg*CNA1* cells that is not observed in wild-type cells. (D) M IES is not eliminated in Δg*CNA1* cells. The upper panel shows schematic drawing of the IES elimination assay of the M element. Primers flanking the M element were used to amplify short M and long M. The expected product sizes are indicated. The lower panel shows the result of the IES elimination assay of M element. WT and Δg*CNA1* cells were assorted to homozygous short M. Whole-cell lysates were prepared from a mass mating of WT or Δg*CNA1* cells at the indicated time postmixing and used for PCR. (E) BES elimination efficiency is greatly reduced in Δg*CNA1* cells. The upper panel shows a schematic drawing of the BES elimination assay of the Tt819 region. Primers flanking the Tt819 region and a primer annealing to telomere sequence were used for nested PCR. The expected product sizes are indicated. The lower panel shows the result of the BES elimination assay of the Tt819 region. Single-cell lysates were prepared from WT and Δg*CNA1* parental cells or from exconjugants 36 h postmixing. WP, wild-type parental cell; WE, wild-type exconjugant; ΔP, Δg*CNA1* parental cell; and ΔE, Δg*CNA1* exconjugant.

cells, the long form was detectable, beginning about 15 h postmixing. In the mating of Δg*CNA1* cells, the long form was never detected (Fig. 6D, lower panel). Therefore, zygotic expression of the *CNA1* gene is required for M element elimination.

We analyzed elimination of the BES-Tt819 element region (45) by PCR of single exconjugants using primers flanking the Tt819 region and one complementary to the telomere DNA sequence (Fig. 6E, upper panel). If BES elimination occurs properly, the primers should amplify two short products, 260 bp for the processed left arm and 140 bp for the right arm. Otherwise, a longer 425-bp product should be amplified. In wild-type cells, BES elimination in the Tt819 region occurred normally (Fig. 6E, lower panel). In Δg*CNA1* progeny cells, these events failed to occur in 9 instances out of 10 examined and occurred inefficiently in 1 case. Therefore, BES elimination is greatly reduced in the mating of Δg*CNA1* cells, as it is in another mutant that effects IES elimination (22).

The zygotic *CNA1* gene is required for the formation of DNA elimination structures. During DNA elimination in *Tetrahymena*, bidirectional micronuclear transcripts containing IESs (7) are processed by a dicer-like protein, Dcl1p, into small interfering RNA-like ~28-nucleotide scan RNAs (scnRNAs) (25). scnRNAs are associated with Twi1p, an Argonaute protein (23), which is required for DNA elimination (22). Two chromodomain-containing programmed DNA degradation proteins (Pdd1p and Pdd3p) are also required for DNA elimination (9, 26). In *Tetrahymena*, histone H3 K9 methylation, a hallmark of heterochromatin, is only found in developing MACs when DNA elimination is occurring (39), and it is dependent on *TWI1* and *DCL1* (17, 25). Eliminating H3 K9 methylation results in failure of DNA elimination (17). In the late stages of NM development, the Pdd proteins and H3 K9 methylation are localized into vesicular electron-dense DNA elimination structures that contain IESs (39).

To understand how *CNA1* affects the DNA elimination pathway, major steps of the pathway were analyzed. During the con-

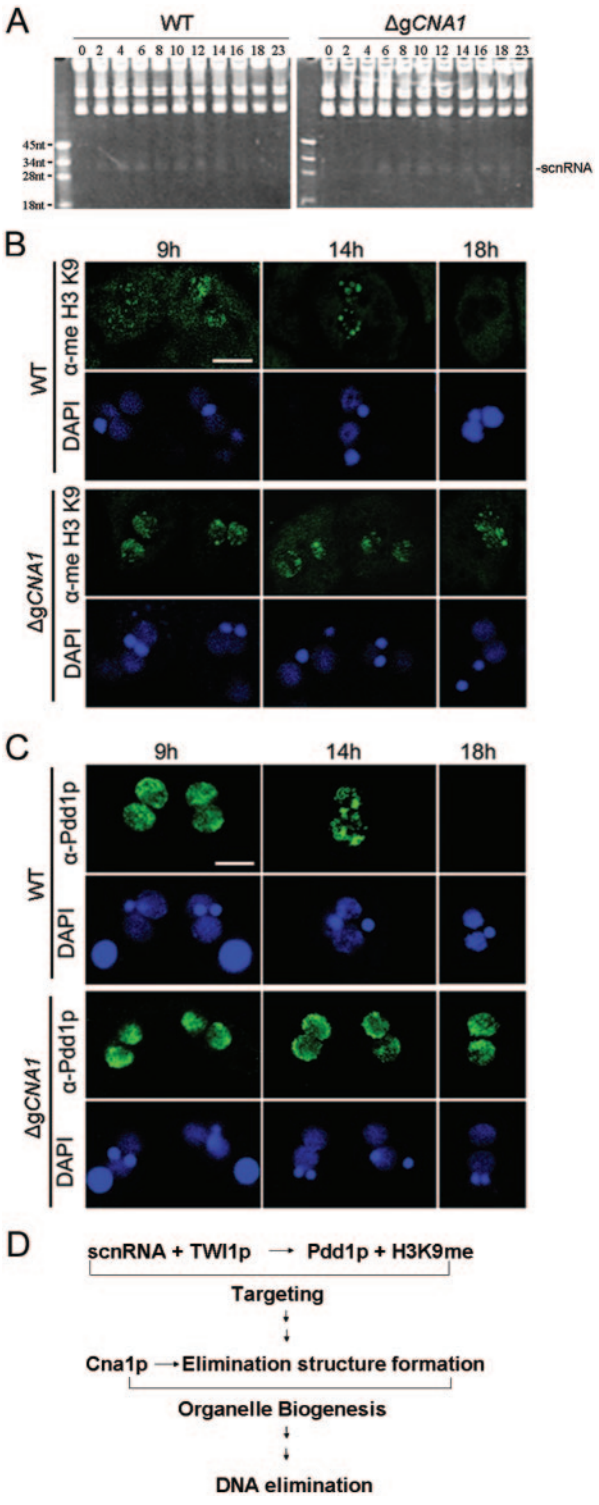

FIG. 7. Analysis of DNA elimination pathway in Δg*CNA1* cells. (A) Accumulation and disappearance of small RNA is not affected in Δg*CNA1* cells. Total RNA was isolated from mating wild-type (WT) or Δg*CNA1* cells at the indicated hours postmixing and separated on gels. DNA oligonucleotides were used as markers. nt, nucleotide. (B) K9-methylated H3 accumulates but does not localize in elimination structures and is not degraded in Δg*CNA1* cells. Mating WT or Δg*CNA1* cells were fixed with Schaudin's fixative at indicated time points postmixing and stained with α-H3 K9 dimethylation antibody (α-me H3 K9). Scale bar, 12 μm. (C) Pdd1 accumulates but does not localize in DNA elimination structures in Δg*CNA1* cells. Mating WT or Δg*CNA1* cells were fixed with Lavdowsky's fixative at the indicated time points and stained with α-Pdd1p antibody. Scale bar, 12 μm. (D) Summary of steps in DNA elimination indicating that Cna1p functions downstream of the targeting process in the DNA elimination pathway.

jugation of Δg*CNA1* cells, accumulation and disappearance of scnRNA occurred normally, albeit slightly more slowly (Fig. 7A), likely due to the fact that conjugation of Δg*CNA1* cells was slower than that of the wild type (see Fig. S2 in the supplemental material). This result suggests that the generation and stability of scnRNA is not affected in Δg*CNA1* cells.

As previously described (39), in wild-type conjugants, H3 K9 dimethylation accumulated in the NMs (Fig. 7B, WT 9 h), became organized into the DNA elimination structures in exconjugants (Fig. 7B, WT 14 h), and disappeared after these structures were eliminated (Fig. 7B, WT 18 h). In contrast, while methylated H3 K9 accumulated in the NMs in Δg*CNA1* conjugants (Fig. 7B, Δg*CNA1* 9 h), it did not become organized into the DNA elimination structures and did not disappear (Fig. 7B, Δg*CNA1* 14 h and 18 h).

Pdd proteins are organized into the DNA elimination structures, and deletions of Pdd proteins result in failure of these structures' formation and of endoreplication (9, 26). Immunostaining of wild-type cells with α-Pdd1p antibody shows Pdd1p first accumulated throughout the NMs in conjugants (Fig. 7C, WT 9 h) and became organized into DNA elimination structures in exconjugants at the 2MAC-2MIC stage (Fig. 7C, WT 14 h). The elimination structures and Pdd1p staining then disappeared (Fig. 7C, WT 18 h). In the NMs of Δg*CNA1* cells, initial accumulation of Pdd1p appeared normal, but Pdd1p-containing DNA elimination structures were never observed (Fig. 7C, Δg*CNA1*), indicating that zygotic expression of *CNA1* is required for the formation of the DNA elimination structures.

DISCUSSION

While the studies described here were in review, a report (6) describing some of the properties of *Tetrahymena CNA1* was published. Some of the results described here confirm or extend the studies reported by Cervantes et al. (6), while others differ. We also studied additional properties of Cna1p. In addition to discussing our data and the areas of agreement between the two studies, we will also attempt to explain the differences.

***CNA1* encodes a centromeric H3 that is essential for vegetative growth.** Both our results and those of Cervantes et al. (6) indicate that Cna1p is a chimeric histone with a H3-like histone fold domain, similar to the CenH3s of other organisms. The micronuclear-specific localization of Cna1p-GFP in small dots whose number correlates closely with the number of micronuclear chromosomes and whose behavior during mitosis is as expected for centromeres argues strongly that Cna1p is the centromeric H3 in *Tetrahymena*.

Knockdown of the *CNA1* gene number in somatic macronuclei resulted in chromosome segregation defects and loss of micronuclear DNA, arguing that Cna1p is required for proper

segregation of mitotic micronuclear chromosomes. It is surprising that complete somatic knockout of the *CNA1* gene was not viable, since micronuclei have no known function in vegetative cells and other mutations that result in severe loss of MIC DNA (25, 40) are not lethal. It is possible that in the other MIC-defective mutants where MICs are very small or nondetectable, only chromosome arms were lost, while minimal centromere regions still remained. It may be the specific loss of centromeres that is responsible for the lethality in *CNA1* knockout cells, possibly because complete loss of centromeres triggers a checkpoint mechanism in growing cells, which can be bypassed as long as centromeres are present and can segregate.

CenH3 deposition during the cell cycle in *Tetrahymena* differs from that of other organisms. In other organisms, deposition of CenH3 can occur at stages of the cell cycle other than S (2). Our studies indicate that, while Cna1p-GFP initially accumulates in the nucleoplasm of M-phase MICs (Fig. 2C), its deposition to centromeres occurs only in S phase (Fig. 3). Because all M-phase MICs exhibited strong nucleoplasmic signal when Cna1p-GFP was first visible shortly after induction of its synthesis (Fig. 3), it is highly likely that Cna1p is synthesized and imported into MICs before S phase in preparation for the following centromere replication, although it could be a "passenger" protein as suggested by Cervantes et al. (6). While it seems likely that deposition of CenH3 in *Tetrahymena* occurs during the micronuclear S phase, we have not determined whether it is always associated with centromere replication per se, since *Tetrahymena* centromere DNA sequences and their precise timing of replication have not yet been identified.

Cna1p localization during early conjugation. Our studies of Cna1p-GFP clearly demonstrate that, when micronuclei begin to elongate at the early stages of meiotic prophase, centromeres are clustered at one end of the MIC, whose morphology indicates it is opposite to where telomeres are clustered (18), and that this organization persists as the meiotic chromosomes elongate and align to form the fully extended crescent (Fig. 4A, b to d).

In addition to centromeric localization, we also observed highly dispersed localization of Cna1p during the meiotic and mitotic divisions using both GFP-tagged Cna1p (Fig. 4) and anti-Cna1p antibody (see Fig. S1 in the supplemental material). Because the GFP signal observed at these stages greatly exceeds the signal observed at centromeres in the preceding stages, this staining likely represents Cna1p that is newly deposited into nuclei rather than disassociation from the centromeres themselves during divisions. The fate of this ectopically localized Cna1p is not clear, but it is likely to be deposited later into newly replicated centromeres, consistent with our observations that a generalized localization of Cna1p also precedes deposition into centromeres in growing cells.

Zygotic *CNA1* is required for the formation of DNA elimination structures. Previous studies on DNA elimination in *Tetrahymena* identified a pathway by which the sequences to be eliminated are first targeted by an RNAi mechanism that is similar to heterochromatin formation in other organisms (for a review, see reference 24). However, little is known about how the deletion-rejoining associated with IESs and the breakage-resection-telomere addition associated with BESs are performed during the later stages of elimination. Pdd proteins are essential for DNA elimination, can be coimmunoprecipitated with IESs, and colocalize with them in subnuclear organelles (DNA elimination structures) in developing MACs (20, 33). Thus, an understanding of the biogenesis and composition of elimination structures is likely to shed light on the later stages of DNA elimination.

We demonstrated that zygotic expression of Cna1p, the CenH3 of *Tetrahymena*, is required for DNA elimination but is not required for essential steps in the targeting process (scnRNA, H3K9 methylation, and Pdd1p association). Rather, zygotic expression of Cna1p appears to be required for the later process of formation of the elimination structures. Consistent with this, we observed weak, diffuse Cna1p localization in NMs around this time using the α-Cna1p antibody (Supplemental material S1). In addition, we observed a small number of cells in which Cna1p antibody staining was associated with DNA elimination structures. This Cna1p localization in DNA elimination structures was not observed in the exconjugants of mating Δg*CNA1* cells (data not shown) or with parental Cna1p-GFP in MCG cells (which have a wild-type background), arguing that the Cna1p in the structures is expressed from the zygotic genome, explaining how the absence of zygotic Cna1p can cause the failure of DNA elimination structure formation in Δg*CNA1* cells.

DNA elimination failure in conjugated Δg*CNA1* cells is not likely due to inducing a checkpoint block. The localization of zygotic expressed Cna1p in DNA elimination structures strongly argues that the DNA elimination failure in conjugated Δg*CNA1* cells is a direct effect of knocking out zygotic *CNA1*. However, an alternative possibility is that lack of zygotic expression of Cna1p may induce a checkpoint response that blocks NM development. Consistent with this idea is the observation that the second endoreplication of the NM genome, which occurs about the same time as DNA elimination in wild-type cells (3), is inhibited during conjugation of Δg*CNA1* cells (Fig. 6C and 7B and C). However, adding aphidicolin during MAC development (10 h postmixing) has been shown to inhibit the second DNA endoreplication without affecting DNA elimination and absorption of one MIC (26). In addition, endoreplication failure has been seen in other DNA elimination mutants, including Pdd1 knockouts, which have been shown to have a direct effect on the RNAi pathway leading to IES elimination.

Another argument that the absence of zygotic expression of Cna1p does not simply induce a checkpoint that blocks progression of conjugation comes from comparison of the phenotypes of different mutant strains with defects in DNA elimination. The progeny of Δg*CNA1* matings are arrested at the 2MAC-2MIC stage, as are other mutants that affect the DNA elimination pathway (9, 22). However, in *TWI1* knockout cells in which scnRNA accumulation and H3 K9 methylation is blocked, the OMs do not degenerate, even at 27 h postmixing (data not shown). In contrast, in conjugating Δg*CNA1* cells, degeneration of the OM occurs normally (see Fig. S2 in the supplemental material). Thus, a block earlier in the scnRNA-mediated elimination process appears to result in a checkpoint-like block in another, subsequent conjugation process (old MAC degeneration), but absence of zygotic Cna1p, which acts after H3 K9 methylation, does not. These observations argue that absence of zygotic Cna1p affects DNA elimination in a more direct manner.

Centromere loci may be initiation sites for formation of DNA elimination structures. We suggest that Cna1p may bind specifically to centromere DNA regions from which the normal complement of centromere proteins has been removed in the developing NM and that this specific binding is required for the initiation of the DNA elimination structure, which is required for efficient elimination of micronuclear limited sequences from the developing NM (Fig. 7D).

Expression of *CNA1* during conjugation. Using Northern blots and reverse transcription-PCR, both we (Fig. 1C and 6B) and Cervantes et al. (6) observed that expression of the *CNA1* gene changes during conjugation. However, using Western blots, Cervantes et al. showed that the total amount of Cna1p remained relatively constant during conjugation (6). These observations indicate that the up-regulation of *CNA1* expression during MIC divisions and DNA elimination do not result in a significant increase of the steady-state level of Cna1p, either because of posttranscriptional or posttranslational control of the *CNA1* gene or because the amounts of Cna1p that are synthesized are small relative to the total amount of Cna1p in the cells.

The localization of centromeres in meiotic crescent nuclei. We observed that Cna1p-GFP-containing centromeres localized at one end of the crescent, opposite the telomeres, during the elongation process and remained at one end when crescents were fully extended (Fig. 4). Cervantes et al. (6) also observed the antipodal organization of centromeres in early prophase but reported that punctate Cna1p then appeared dispersed throughout the fully extended crescent nucleus, and they could not distinguish the position of intact centromeres (Fig. 4 in reference 6) at later crescent stages. We believe this discrepancy reflects differences in the methods used to detect Cna1p. Cervantes et al. used antibodies to Cna1p (6), and the epitope that the antibody recognizes could be more exposed on Cna1p molecules that are in the nucleoplasm, causing them to stain more intensely than centromeric Cna1p and making it appear that Cna1p had delocalized from the centromeres. We utilized GFP-tagged Cna1p, which might be expected to fluoresce the same regardless of the location of the protein, enabling the centromere-associated Cna1p-GFP to be detected easily.

The effect of zygotic *CNA1* expression on DNA elimination. In contrast to our observation that exconjugants of mating Δg*CNA1* cells were arrested at the 2MAC-2MIC stage and eventually died, Cervantes et al. found that the progeny of mating of Δg*CNA1* cells were viable and could divide for a few generations (6). To understand why the Δg*CNA1* cells created in the two laboratories exhibit such differences, we compared the immunofluorescent staining in the two studies. Cervantes et al. observed that Cna1p staining in the NMs was as intense as that observed during the preceding meiosis and mitoses, and that this strong parental staining persisted until the time of DNA elimination, about 12 h postmixing (6). In our cells, the parental Cna1p level decreased much earlier, about 7 h postmixing, when the NMs started to differentiate (see Fig. S1 in the supplemental material). Therefore, the strains that Cervantes et al. used appear to have higher levels of parental Cna1p than our strains. This additional Cna1p could have been sufficient to allow cells to perform DNA elimination and give rise to viable progeny. It is likely that our cells, having less parental Cna1p, required expression from the zygotic *CNA1* gene for the formation of DNA elimination structures, which is also required for subsequent development of the exconjugants. Cervantes et al. also did not observe Cna1p in the DNA elimination structures (6). We only observed Cna1p in the DNA elimination structures in a small fraction of cells, indicating that Cna1p is only present in these structures for a very short time. In addition, the intense signal they observed from the larger amounts of parental Cna1p in the NMs in their strains could have obscured the signal in the DNA elimination structures. Thus, we believe that it is strain variation that caused the different phenotypes between the cells studied by the two laboratories. These considerations suggest that Cna1p is required for DNA elimination and production of viable progeny in *Tetrahymena* but that expression of zygotic Cna1p is only required in the absence of sufficient parental Cna1p. Other examples of strain variation in gene expression have been seen in different strains of *Tetrahymena* (T. Noto and M. A. Gorovsky, unpublished observations).

ACKNOWLEDGMENTS

We thank Kazufumi Mochizuki for helpful discussions and assistance with experimental protocols. We thank Marcella Cervantes, Meng-Chao Yao, and Harmit Malik for the α-Cna1p antibody.

This work was supported by grant GM21793 from the NIH.

REFERENCES

1. **Ahmad, K., and S. Henikoff.** 2001. Centromeres are specialized replication domains in heterochromatin. J. Cell Biol. **153:**101–110.
2. **Ahmad, K., and S. Henikoff.** 2002. Histone H3 variants specify modes of chromatin assembly. Proc. Natl. Acad. Sci. USA **99**(Suppl. 4)**:**16477–16484.
3. **Austerberry, C. F., C. D. Allis, and M. C. Yao.** 1984. Specific DNA rearrangements in synchronously developing nuclei of Tetrahymena. Proc. Natl. Acad. Sci. USA **81:**7383–7387.
4. **Black, B. E., D. R. Foltz, S. Chakravarthy, K. Luger, V. L. Woods, Jr., and D. W. Cleveland.** 2004. Structural determinants for generating centromeric chromatin. Nature **430:**578–582.
5. **Cassidy-Hanley, D., J. Bowen, J. H. Lee, E. Cole, L. A. VerPlank, J. Gaertig, M. A. Gorovsky, and P. J. Bruns.** 1997. Germline and somatic transformation of mating Tetrahymena thermophila by particle bombardment. Genetics **146:**135–147.
6. **Cervantes, M. D., X. Xi, D. Vermaak, M. C. Yao, and H. S. Malik.** 2006. The CNA1 histone of the ciliate Tetrahymena thermophila is essential for chromosome segregation in the germline micronucleus. Mol. Biol. Cell **17:**485–497.
7. **Chalker, D. L., and M. C. Yao.** 2001. Nongenic, bidirectional transcription precedes and may promote developmental DNA deletion in Tetrahymena thermophila. Genes Dev. **15:**1287–1298.
8. **Chikashige, Y., D. Q. Ding, H. Funabiki, T. Haraguchi, S. Mashiko, M. Yanagida, and Y. Hiraoka.** 1994. Telomere-led premeiotic chromosome movement in fission yeast. Science **264:**270–273.
9. **Coyne, R. S., M. A. Nikiforov, J. F. Smothers, C. D. Allis, and M. C. Yao.** 1999. Parental expression of the chromodomain protein Pdd1p is required for completion of programmed DNA elimination and nuclear differentiation. Mol. Cell **4:**865–872.
10. **Davidson, L., and J. R. LaFountain, Jr.** 1975. Mitosis and early meiosis in Tetrahymena pyriformis and the evolution of mitosis in the phylum Ciliophora. Biosystems **7:**326–336.1975.
11. **Doerder, F. P., and L. E. Debault.** 1975. Cytofluorimetric analysis of nuclear DNA during meiosis, fertilization and macronuclear development in the ciliate Tetrahymena pyriformis, syngen 1. J. Cell Sci. **17:**471–493.
12. **Gaertig, J., L. Gu, B. Hai, and M. A. Gorovsky.** 1994. High frequency vector-mediated transformation and gene replacement in Tetrahymena. Nucleic Acids Res. **22:**5391–5398.
13. **Gorovsky, M. A., M. C. Yao, J. B. Keevert, and G. L. Pleger.** 1975. Isolation of micro- and macronuclei of Tetrahymena pyriformis. Methods Cell Biol. **9:**311–327.
14. **Hai, B., and M. A. Gorovsky.** 1997. Germ-line knockout heterokaryons of an essential alpha-tubulin gene enable high-frequency gene replacement and a test of gene transfer from somatic to germ-line nuclei in Tetrahymena thermophila. Proc. Natl. Acad. Sci. USA **94:**1310–1315.
15. **Henikoff, S., and Y. Dalal.** 2005. Centromeric chromatin: what makes it unique? Curr. Opin. Genet. Dev. **15:**177–184.

16. **Karrer, K. M.** 2000. Tetrahymena genetics: two nuclei are better than one. Methods Cell Biol. **62:**127–186.
17. **Liu, Y., K. Mochizuki, and M. A. Gorovsky.** 2004. Histone H3 lysine 9 methylation is required for DNA elimination in developing macronuclei in Tetrahymena. Proc. Natl. Acad. Sci. USA **101:**1679–1684.
18. **Loidl, J., and H. Scherthan.** 2004. Organization and pairing of meiotic chromosomes in the ciliate Tetrahymena thermophila. J. Cell Sci. **117:**5791–5801.
19. **Madireddi, M. T., M. C. Davis, and C. D. Allis.** 1994. Identification of a novel polypeptide involved in the formation of DNA-containing vesicles during macronuclear development in Tetrahymena. Dev. Biol. **165:**418–431.
20. **Madireddi, M. T., R. S. Coyne, J. F. Smothers, K. M. Mickey, M. C. Yao, and C. D. Allis.** 1996. Pdd1p, a novel chromodomain-containing protein, links heterochromatin assembly and DNA elimination in Tetrahymena. Cell **87:**75–84.
21. **Mellone, B. G., and R. C. Allshire.** 2003. Stretching it: putting the CEN(P-A) in centromere. Curr. Opin. Genet. Dev. **13:**191–198.
22. **Mochizuki, K., N. A. Fine, T. Fujisawa, and M. A. Gorovsky.** 2002. Analysis of a piwi-related gene implicates small RNAs in genome rearrangement in tetrahymena. Cell **110:**689–699.
23. **Mochizuki, K., and M. A. Gorovsky.** 2004. Conjugation-specific small RNAs in Tetrahymena have predicted properties of scan (scn) RNAs involved in genome rearrangement. Genes Dev. **18:**2068–2073.
24. **Mochizuki, K., and M. A. Gorovsky.** 2004. Small RNAs in genome rearrangement in Tetrahymena. Curr. Opin. Genet. Dev. **14:**181–187.
25. **Mochizuki, K., and M. A. Gorovsky.** 2005. A Dicer-like protein in Tetrahymena has distinct functions in genome rearrangement, chromosome segregation, and meiotic prophase. Genes Dev. **19:**77–89.
26. **Nikiforov, M. A., J. F. Smothers, M. A. Gorovsky, and C. D. Allis.** 1999. Excision of micronuclear-specific DNA requires parental expression of pdd2p and occurs independently from DNA replication in Tetrahymena thermophila. Genes Dev. **13:**2852–2862.
27. **Pollard, T. D., and W. C. Earnshaw.** 2002. Cell biology. Saunders, Philadelphia, Pa.
28. **Sarma, K., and D. Reinberg.** 2005. Histone variants meet their match. Nat. Rev. Mol. Cell. Biol. **6:**139–149.
29. **Shang, Y., X. Song, J. Bowen, R. Corstanje, Y. Gao, J. Gaertig, and M. A. Gorovsky.** 2002. A robust inducible-repressible promoter greatly facilitates gene knockouts, conditional expression, and overexpression of homologous and heterologous genes in Tetrahymena thermophila. Proc. Natl. Acad. Sci. USA **99:**3734–3739.
30. **Sharp, J. A., and P. D. Kaufman.** 2003. Chromatin proteins are determinants of centromere function. Curr. Top. Microbiol. Immunol. **274:**23–52.
31. **Shelby, R. D., K. Monier, and K. F. Sullivan.** 2000. Chromatin assembly at kinetochores is uncoupled from DNA replication. J. Cell Biol. **151:**1113–1118.
32. **Smith, M. M.** 2002. Centromeres and variant histones: what, where, when and why? Curr. Opin. Cell Biol. **14:**279–285.
33. **Smothers, J. F., C. A. Mizzen, M. M. Tubbert, R. G. Cook, and C. D. Allis.** 1997. Pdd1p associates with germline-restricted chromatin and a second novel anlagen-enriched protein in developmentally programmed DNA elimination structures. Development **124:**4537–4545.
34. **Sullivan, B., and G. Karpen.** 2001. Centromere identity in Drosophila is not determined in vivo by replication timing. J. Cell Biol. **154:**683–690.
35. **Sullivan, B. A., M. D. Blower, and G. H. Karpen.** 2001. Determining centromere identity: cyclical stories and forking paths. Nat. Rev. Genet. **2:**584–596.
36. **Sullivan, K. F.** 2001. A solid foundation: functional specialization of centromeric chromatin. Curr. Opin. Genet. Dev. **11:**182–188.
37. **Sullivan, K. F., M. Hechenberger, and K. Masri.** 1994. Human CENP-A contains a histone H3 related histone fold domain that is required for targeting to the centromere. J. Cell Biol. **127:**581–592.
38. **Talbert, P. B., T. D. Bryson, and S. Henikoff.** 2004. Adaptive evolution of centromere proteins in plants and animals. J. Biol. **3:**18.
39. **Taverna, S. D., R. S. Coyne, and C. D. Allis.** 2002. Methylation of histone h3 at lysine 9 targets programmed DNA elimination in tetrahymena. Cell **110:**701–711.
40. **Wei, Y., L. Yu, J. Bowen, M. A. Gorovsky, and C. D. Allis.** 1999. Phosphorylation of histone H3 is required for proper chromosome condensation and segregation. Cell **97:**99–109.
41. **Wieland, G., S. Orthaus, S. Ohndorf, S. Diekmann, and P. Hemmerich.** 2004. Functional complementation of human centromere protein A (CENP-A) by Cse4p from *Saccharomyces cerevisiae*. Mol. Cell. Biol. **24:**6620–6630.
42. **Wilson, E. B.** 1928. The cell in development and heredity, 3rd edition. Macmillan, New York, N.Y.
43. **Woodard, J., E. Kaneshiro, and M. A. Gorovsky.** 1972. Cytochemical studies on the problem of macronuclear subnuclei in Tetrahymena. Genetics **70:**421–431.
44. **Wu, M., C. D. Allis, and M. A. Gorovsky.** 1988. Cell-cycle regulation as a mechanism for targeting proteins to specific DNA sequences in Tetrahymena thermophila. Proc. Natl. Acad. Sci. USA **85:**2205–2209.
45. **Yao, M. C., K. Zheng, and C. H. Yao.** 1987. A conserved nucleotide sequence at the sites of developmentally regulated chromosomal breakage in Tetrahymena. Cell **48:**779–788.